Simulating twistronics in acoustic metamaterials

S. Minhal Gardezi,[1] Harris Pirie,[2] Stephen Carr,[3] William Dorrell,[2] and Jennifer E. Hoffman[1,2,*]

[1] *School of Engineering and Applied Sciences, Harvard University, Cambridge, MA, 02138, USA*
[2] *Department of Physics, Harvard University, Cambridge, MA, 02138, USA*
[3] *Brown Theoretical Physics Center and Department of Physics, Brown University, Providence, RI, 02912-1843, USA*

(Dated: March 24, 2021)

Twisted van der Waals (vdW) heterostructures have recently emerged as a tunable platform for studying correlated electrons. However, these materials require laborious and expensive effort for both theoretical and experimental exploration. Here we numerically simulate twistronic behavior in acoustic metamaterials composed of interconnected air cavities in two stacked steel plates. Our classical analog of twisted bilayer graphene perfectly replicates the band structures of its quantum counterpart, including mode localization at a magic angle of 1.12°. By tuning the thickness of the interlayer membrane, we reach a regime of strong interlayer tunneling where the acoustic magic angle appears as high as 6.01°, equivalent to applying 130 GPa to twisted bilayer graphene. In this regime, the localized modes are over five times closer together than at 1.12°, increasing the strength of any emergent non-linear acoustic couplings.

INTRODUCTION

1 Van der Waals (vdW) heterostructures host a diverse set of useful emergent properties that can be customized by varying the stacking configuration of sheets of two-dimensional (2D) materials, such as graphene, other xenes, or transition-metal dichalcogenides [1–4]. Recently, the possibility of including a small twist angle between adjacent layers in a vdW heterostructure has led to the growing field of twistronics [5]. The twist angle induces a moiré pattern that acts as a tunable potential for electrons moving within the layers, promoting enhanced electron correlations when their kinetic energy is reduced below their Coulomb interaction. Even traditional non-interacting materials can reach this regime, as exemplified by the correlated insulating state in twisted bilayer graphene [6]. Already, vdW heterostructures with moiré superlattices have led to new platforms for Wigner crystals [7], interlayer excitons [8–10], and unconventional superconductivity [11–13]. But the search for novel twistronic phases is still in its infancy and there are countless vdW stacking and twisting arrangements that remain unexplored. Theoretical investigations of these new arrangements are limited by the large and complex moiré patterns created by multiple small twist angles. Meanwhile, fabrication of vdW heterostructures is restricted to the symmetries and properties of the few free-standing monolayers available today. It remains pressing to develop a more accessible platform to rapidly prototype and explore new twistronic materials to accelerate their technological advancement.

2 The development of acoustic metamaterials over the last few years has unlocked a compelling platform to guide the design of new quantum materials [14]. Whereas quantum materials can be difficult to predict and fabricate, acoustic metamaterials have straightforward governing equations, continuously tunable properties, fast build times, and inexpensive characterization tools, making them attractive testbeds to rapidly explore their quantum counterparts. Sound waves in an acoustic metamaterial can be reshaped to mimic the collective motion of electrons in a crystalline solid. These acoustic devices can recreate many phenomena seen in quantum materials, such as chiral Landau levels [15], higher-order topology [16, 17], and fragile topology [18]. In vdW systems, the Dirac-like electronic bands in graphene have been mimicked using longitudinal acoustics [19–21], surface acoustic waves [22], and mechanics [23, 24]. Further, it was recently discovered that placing a thin membrane between metamaterial layers can reproduce the coupling effects of vdW forces, yielding acoustic analogs of bilayer and trilayer graphene [25, 26]. The inclusion of a twist angle between metamaterial layers has the potential to further expand their utility. In addition to electronic systems, moiré engineering has recently been demonstrated in systems containing vibrating plates [27], spoof surface-acoustic waves [28], and optical lattices [29]. However, without simultaneous control of in-plane hopping, interlayer coupling, and twist angle, rapidly prototyping next-generation twistronic devices using acoustic metamaterials remains an elusive goal.

3 Here we propose a simple acoustic metamaterial that precisely recreates the band structure of twisted bilayer graphene, including mode localization at a magic angle of 1.12°. We start with a monolayer acoustic metamaterial that implements a tight-binding model describing the low-energy band structure of graphene. By combining two of these monolayers with an intermediate polyethylene membrane, we numerically simulate both stacking configurations of *untwisted* bilayer graphene using finite-element modeling software, COMSOL MULTIPHYSICS. Our simulated acoustic analog of *twisted* bilayer graphene hosts flat bands at the same magic angle of $\sim 1.1°$ as its quantum counterpart [6, 30]. A key

* jhoffman@physics.harvard.edu

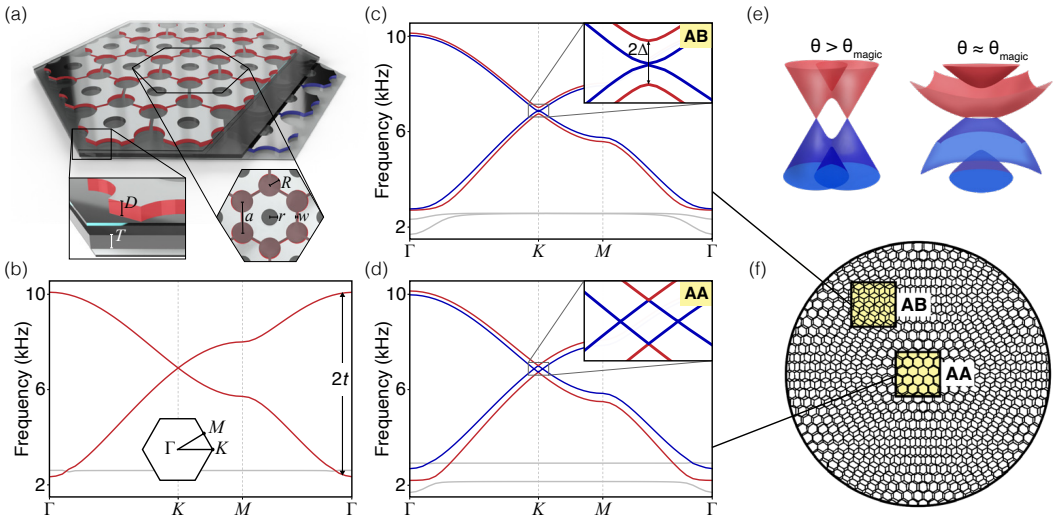

FIG. 1. Acoustic vdW metamaterials. (a) In this acoustic metamaterial, sound waves propagate through connected air cavities in solid steel to mimic the way that electrons hop between carbon atoms in bilayer graphene. Our metamaterial design has cavity spacing $a = 10$ mm, cavity radius $R = 3.5$ mm, channel width $w = 0.875$ mm, and steel thickness $D = 1$ mm. The smaller, unconnected cavities in the center of each unit cell improve the interlayer coupling of our bilayer metamaterial, but they do not act as additional lattice sites. (b) The C_6 symmetry of the lattice protects a Dirac-like crossing at the K point of the calculated monolayer acoustic band structure. (c-d) Two sheets of acoustic graphene coupled by an interlayer polyethylene membrane of thickness $T = 2.35$ mm accurately recreate the AB and AA configurations of bilayer graphene, as shown in these calculations. (e) As the two sheets are twisted relative to one another, the two Dirac cones contributed by each layer hybridize, ultimately producing a flat band at small twist angles. (f) The twisted bilayer heterostructure has its own macroscopic periodicity with distinct AB and AA stacking regions.

advantage of our metamaterial is the ease with which it reaches coupling conditions beyond those feasible in atomic bilayer graphene. By tuning the thickness of the interlayer membrane, we design new metamaterials that host flat bands at several magic angles between 1.12° and 6.01°. Our results demonstrate the potential for acoustic vdW metamaterials to precisely simulate and explore the ever-growing number of quantum twistronic materials.

RESULTS AND DISCUSSION

4 We begin by introducing a general framework for designing acoustic metamaterials to prototype non-interacting electronic materials that are well described by a tight-binding model. In our metamaterial, each atomic site is represented by a cylindrical air cavity in a steel plate (see Fig. 1(a)). The radius of the air cavity determines the eigenfrequencies of its ladder of acoustic standing modes. In a lattice of these cavities, the degenerate standing modes form narrow bands, separated from each other by a large frequency gap. We focus primarily on the lowest, singly degenerate s band. Just as electrons hop from atom to atom in an electronic tight-binding model, sound waves propagate from cavity to cavity in our acoustic metamaterial through a network of tunable thin air channels. This coupling is always positive for s cavity modes, but either sign can be realized by starting with higher-order cavity modes [31]. Because sound travels much more easily through air than through steel, these channels are the dominant means of acoustic transmission through our metamaterial. They allow nearest- and next-nearest-neighbor coupling to be controlled independently by varying the width or length of separate air channels, providing a platform to implement a broad class of tight-binding models.

5 To recreate bilayer graphene in an acoustic metamaterial, we started from a honeycomb lattice of air cavities, with radius of 3.5 mm and a separation of 10 mm, in a 1-mm-thick steel sheet, encapsulated by 1-mm-thick polyethylene boundaries. Each cavity is coupled to its three nearest neighbors using 0.875-mm-wide channels, giving an s-mode bandwidth of $2t = 7.8$ kHz (see Fig. 1(b)). This s manifold is well isolated from other higher-order modes in the lattice, which appear above 25 kHz. The C_6 symmetry of our metamaterial ensures a linear crossing at the K point, similar to the Dirac cone in graphene [32]. The frequency of this Dirac-like crossing and other key aspects of the band structure are controlled by the dimensions of the cavities and channels. Building on previous work, we coupled two layers of acoustic graphene together using a thin interlayer membrane [26]. By laterally translating the stacking configuration, the same acoustic metamaterial mimics both the parabolic touching around the K point seen in AB-stacked bilayer graphene, and the offset Dirac bands seen in AA-stacked bilayer graphene [33, 34], as shown in Fig. 1(c-d). The frequency span between the K-point eigenmodes is twice

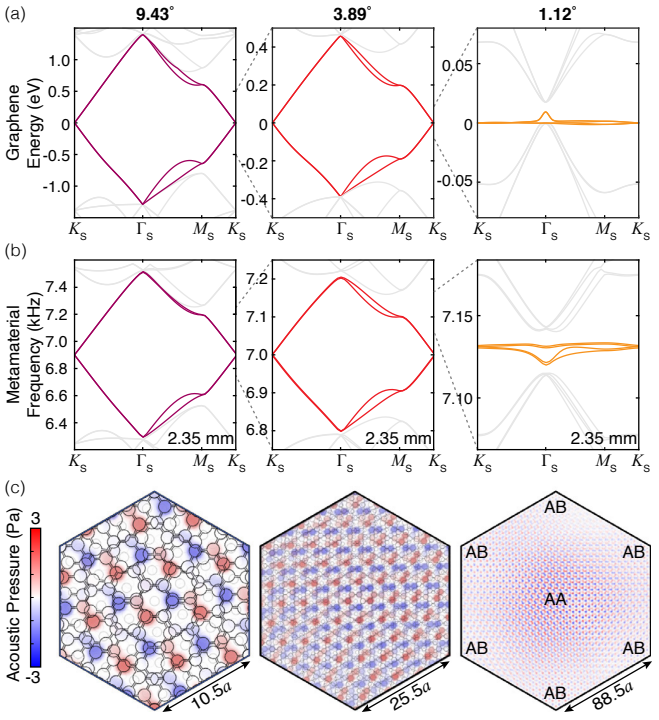

FIG. 2. Trapping sound by twisting. (a) As the twist angle between two layers of graphene decreases, the Dirac bands are compressed around the Fermi level, eventually becoming completely flat at a magic angle of 1.12°, as shown in these electronic tight-binding calculations of unrelaxed twisted bilayer graphene. (b) The same trend occurs in our numerical simulations of a bilayer acoustic metamaterial, spawning acoustic flat bands at 1.12°. (c) For large angles, the calculated acoustic Dirac-like modes at the K_s point are itinerant and persist across the entire supercell. But at the magic angle, they become localized on the AA-stacked region in the center of the supercell.

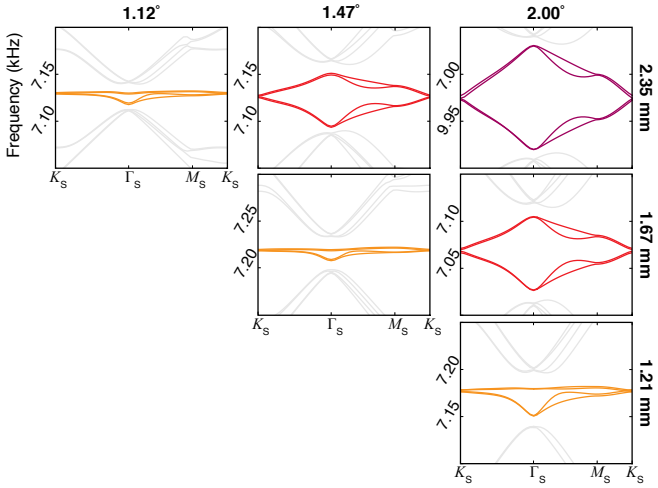

FIG. 3. Interlayer coupling tunes the magic angle. Reducing the thickness of the polyethylene membrane enhances the coupling between layers of our simulated acoustic metamaterial. Consequently, an acoustic flat band (orange) can been formed either by decreasing the twist angle with a fixed membrane thickness (along rows), or by decreasing the thickness at fixed angle (columns). For example, to realize flat bands at 2°, we need to reduce the membrane thickness to 1.21 mm.

the interlayer coupling strength Δ, which is set by the interlayer membrane thickness [26]. We found that a 2.35-mm-thick polyethylene membrane (density 950 kg/m^3 and speed of sound 2460 m/s) accurately matched the dimensionless coupling ratio $\Delta/t \approx 5\%$ in bilayer graphene.

6 Introducing a twist angle between two graphene layers creates a moiré pattern that grows in size as the angle decreases. At small angles, the Dirac cones from each layer are pushed together and hybridize due to the interlayer coupling [35, 36], as shown in Fig. 1(e). Eventually, they form a flat band with a vanishing Fermi velocity (v_F) at a so-called magic angle [6, 30, 37], see Fig. 2(a). We searched for the same band-flattening mechanism by introducing a commensurate-angle twist to our acoustic bilayer graphene metamaterial. Strikingly, our metamaterial mimics its quantum counterpart even down to the magic angle, producing acoustic flat bands at 1.12°, as shown in Fig. 2(a-b). Importantly, there are no other acoustic bands near the Dirac point that can fold and interfere with these flat bands (see Fig. 1(b)). The flat bands appear upside down in our acoustic model because its interlayer coupling (between s cavity modes) has the opposite sign from graphene's (between p_z orbitals). However, this asymmetry is quite small and its influence is not generally noticeable at higher angles [30, 38]. Our acoustic flat bands correspond to real-space pressure modes that are primarily located on the AA region, see Fig. 2(c). This AA localization agrees with calculations of the local electronic density of states in magic-angle twisted bilayer graphene [6, 39]. In our acoustic system, these localized modes represent sound waves that propagate with a low group velocity of 0.05 m/s, compared to 30 m/s in the untwisted bilayer.

7 The magic angle of twisted bilayer graphene can be tuned by applying vertical pressure to push the graphene layers closer together and increase the interlayer coupling [40]. Consequently, the Dirac bands begin to flatten at higher angles under pressure than at ambient conditions. However, a substantial vertical pressure of a few GPa is required to move the magic angle from 1.1° to 1.27°, corresponding to only a 20% increase in the interlayer coupling strength [12]. In our metamaterial, no such physical restrictions apply: the interlayer coupling can be tuned over two orders of magnitude simply by changing the thickness of the coupling membrane [26]. In practice, we anticipate an experimental setup that includes interchangeable polyethylene sheets of different thicknesses. To demonstrate this capability, we numerically reproduced the band flattening at a fixed angle of 2° simply by incrementally reducing the thickness of the interlayer membrane to 1.21 mm (Fig. 3). In other words, the flat band condition can be approached from two directions:

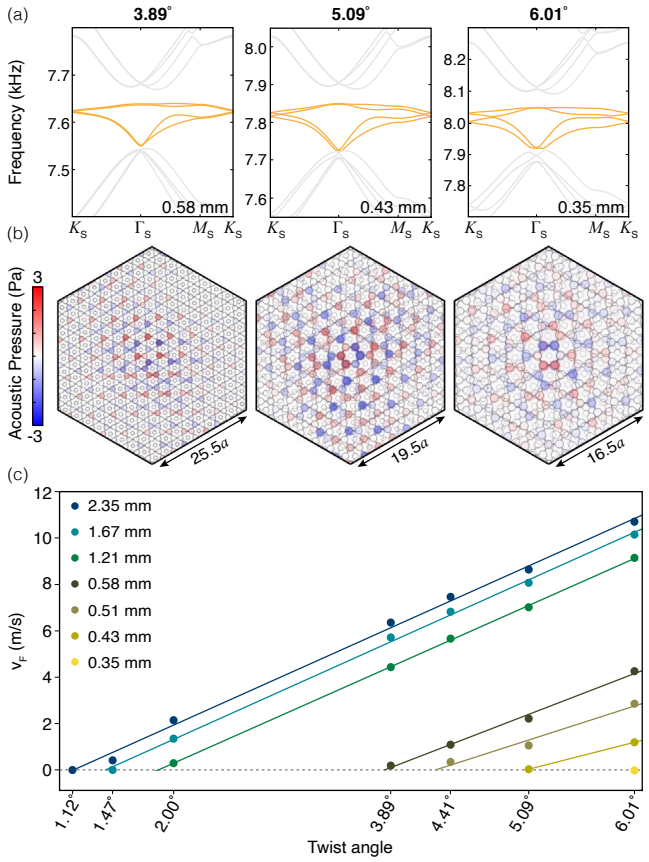

FIG. 4. Reproducing flat bands at high magic angles. (a) By reducing the thickness of the interlayer membrane to 0.58 mm, 0.43 mm, and 0.35 mm, we computed flat bands at 3.89°, 5.09°, and 6.01° twist angles. (b) In each case, the simulated K_s-point eigenmodes appear predominantly around the AA-stacked region in the center of the supercell. As the supercell shrinks, these localized modes form a dense array, increasing the possibility of interactions with similar localized modes in neighboring supercells. (c) By correctly choosing the interlayer membrane's thickness, any angle can become a magic angle with a vanishing K_s-point velocity.

either reduce the twist angle at fixed interlayer thickness, or reduce the thickness at fixed angle. For comparison, it is expected to require about 9 GPa of vertical pressure for twisted bilayer graphene to reach flat bands at 2° [40].

8 Our acoustic metamaterial provides a simple computational platform to explore twistronics in extreme coupling regimes, well beyond the experimental capability of its electronic counterpart. By further reducing the interlayer membrane thickness, we searched for flat bands at high commensurate angles of 3.89°, 5.09°, and 6.01°, equivalent to pressures of 45 GPa, 85 GPa, and 129 GPa that would need to be applied to the graphene system [40]. In each case, we discovered flat bands similar to those in twisted bilayer graphene (Fig. 4(a)). These flat bands all correspond to collective pressure modes that are localized on the AA-stacked central regions (Fig. 4(b)). But these localized modes are over five times closer to each other spatially at 6.01° than they are at 1.12°. Generally speaking, the modes interact more strongly as they become closer together, potentially allowing interactions to dominate over the reduced kinetic energy at a high magic angle. Consequently, a high-magic-angle metamaterial could be susceptible to non-linear effects if tuned correctly, akin to a phonon-phonon interaction. In principle, any twist angle can become a magic angle that hosts a dense array of such localized modes, by choosing the correct interlayer thickness (Fig. 4(c)).

9 Although we focused on recreating twisted bilayer graphene, our metamaterial can be easily extended to capture other vdW systems. For example, by breaking the sublattice symmetry in our unit cell, one can explore the localized modes shaped from twisted quadratic bands, imitating semiconductors like hexagonal boron nitride [41] or transition-metal dichalcogenides [42]. Our metamaterial platform could even mimic twistronic Hamiltonians that cannot yet be realized in condensed matter experiments, which are restricted to the primarily-hexagonal set of 2D materials available today. In principle, a twistronic heterostructure can be constructed from any lattice symmetry to spawn diverse flat bands with distinct topologies [43]. Acoustic metamaterials can smoothly deform between these twistronic phases, allowing their properties to be isolated, optimized, or combined. Further, our metamaterial design can independently control AA and AB coupling by appropriately texturing the interlayer membrane, which may unlock perfectly flat bands at the magic angle [44]. It can also implement tunable in-plane lattice relaxation, which modifies both the electronic [45, 46] and phononic [47, 48] bands in twisted bilayer graphene. Beyond two-layer systems, our design motivates a future experimental setup to explore the intricate moiré patterns created by multiple arbitrary twist angles. Such experimental acoustic devices may quickly surpass theoretical electronic calculations, which are made nearly impossible by the highly incommensurate geometry, even in the three-layer case [49]. Importantly, our design translates to the length scales and materials required for photonic [19] or surface-acoustic-wave [22] devices, which may provide a more-natural platform to fabricate the large arrays required to study complex multilayer structures.

CONCLUSION

10 The enormous phase space of twisted vdW heterostructures promises many new phenomena, but unearthing them is hindered by theoretical and experimental obstacles. Our twisted bilayer metamaterial translates the field of twistronics to acoustics, opening a different path to continue this search (see roadmap in supplement). By introducing a twist angle to vdW metamaterials, we discovered flat bands that *precisely* mimic the behavior of twisted bilayer graphene at 1.1° and that slow transmitted sound by a factor of 600 (20 times slower

than a leisurely walk). The close agreement between our acoustic system and its electronic counterpart gives confidence that twisted acoustic metamaterials can be a valuable platform for more general quantum material design. For example, future 3D-printed acoustic metamaterials could simulate multilayer twistronic heterostructures containing several independent twist angles, a challenging regime for today's theoretical tools. Meanwhile, recent experiments have demonstrated control of surface acoustic waves in the quantum limit [50, 51], which could provide a new direction to incorporate phonon-phonon interactions into our acoustic system.

METHODS

We simulate three-dimensional metamaterial models using the pressure acoustics, frequency domain interface within the acoustics module of COMSOL MULTIPHYSICS. A basic monolayer metamaterial consists of a honeycomb arrangement of air cavities, with radius of 3.5 mm and a separation of 10 mm, in a 1-mm-thick steel sheet. To form a bilayer metamaterial, two such steel sheets are separated and bounded by three identical polyethylene membranes, as shown in Fig. 1(a). The bounding and interlayer membranes all have identical, tunable thicknesses. Each model is cut to form a supercell at a commensurate twist angle, allowing three pairs of Floquet periodic boundary conditions on its six hexagonal sides. The top and bottom boundary sheets are impedance-matched to air on their outer faces. Our metamaterial contains three materials: steel plates (density 7070 kg/m^3 and speed of sound 5790 m/s), air cavities (1.2 kg/m^3, 343 m/s), and high-density polyethylene interlayer and outer boundary membranes (950 kg/m^3, 2460 m/s). The mesh conditions we use depend on the size of the unit cell. For the monolayer and untwisted bilayer metamaterials, as well as twisted bilayer metamaterials with twist angles above 3.89°, we use the physics-controlled "fine" mesh. For models with lower twist angles, we switch to a coarser user-defined mesh with the following parameters: minimum element size 0.09, maximum element size 1, maximum growth rate 1.45, curvature factor 0.5, and resolution 0.6. After constructing the appropriate metamaterial supercell, we create an eigenfrequency study using the following parametric sweep. For a hexagonal supercell with moiré length L, we simulate the $\mathbf{k}$-space sweep around the supercell Brillouin zone along the path $\Gamma_s \to K_s \to M_s \to \Gamma_s$ using the following equation:

$$\mathbf{k} = \frac{\pi}{3\sqrt{3}L} \begin{cases} \begin{pmatrix} 4a \\ 0 \end{pmatrix} & 0 < a < 1 \\ \begin{pmatrix} 6 - 2a \\ \sqrt{3}(2a-1) \end{pmatrix} & 1 < a < 1.5 \\ \begin{pmatrix} 3 + 3\sqrt{3} - 2\sqrt{3}a \\ 3 + \sqrt{3} - 2a \end{pmatrix} & 1.5 < a < \dfrac{3+\sqrt{3}}{2}, \end{cases}$$

where a is an arbitrary sweep parameter. To speed up computation, we typically calculate only the ten eigenfrequencies closest to the Dirac frequency.

The electronic band structures of TBG displayed in Fig. 2(a) were generated using a tight-binding model based on density functional theory (DFT) results for bilayer graphene [52]. For the selected angles, we use a twisted commensurate supercell alongside the DFT-derived couplings to populate an electronic k-dependent Hamiltonian, which we then diagonalize. Although atomic relaxations are known to modify the magic angle and the low-energy band gaps between the flat bands and nearby bands in quantum materials [38], we do not attempt to incorporate analogous relaxations in our metamaterial.

ACKNOWLEDGEMENTS

We thank Alex Kruchkov, Haoning Tang, Clayton DeVault, Daniel Larson, Nathan Drucker, Ben November, Walker Gillett, and Fan Du for insightful discussions. The computations in this paper were run on the FASRC Cannon cluster supported by the FAS Division of Science Research Computing Group at Harvard University. This work was supported by the National Science Foundation Grant No. OIA-1921199 and the Science Technology Center for Integrated Quantum Materials Grant No. DMR-1231319. W.D. acknowledges support from a Herchel Smith Scholarship.

[1] S.-J. Liang, B. Cheng, X. Cui, and F. Miao, Van der Waals Heterostructures for High-Performance Device Applications: Challenges and Opportunities, Advanced Materials **32**, 1903800 (2020).
[2] A. K. Geim and I. V. Grigorieva, Van der Waals heterostructures, Nature **499**, 419 (2013).
[3] P. Ajayan, P. Kim, and K. Banerjee, Two-dimensional van der Waals materials, Physics Today **69**, 38 (2016).
[4] K. S. Novoselov, A. Mishchenko, A. Carvalho, and A. H. Castro Neto, 2D materials and van der Waals heterostructures, Science **353**, aac9439 (2016).
[5] S. Carr, D. Massatt, S. Fang, P. Cazeaux, M. Luskin, and E. Kaxiras, Twistronics: Manipulating the electronic properties of two-dimensional layered structures through their twist angle, Physical Review B **95**, 075420 (2017).
[6] Y. Cao, V. Fatemi, A. Demir, S. Fang, S. L. Tomarken, J. Y. Luo, J. D. Sanchez-Yamagishi, K. Watanabe, T. Taniguchi, E. Kaxiras, R. C. Ashoori, and P. Jarillo-Herrero, Correlated insulator behaviour at half-filling in magic-angle graphene superlattices, Nature **556**, 80

(2018).
[7] E. C. Regan, D. Wang, C. Jin, M. I. Bakti Utama, B. Gao, X. Wei, S. Zhao, W. Zhao, Z. Zhang, K. Yumigeta, M. Blei, J. D. Carlström, K. Watanabe, T. Taniguchi, S. Tongay, M. Crommie, A. Zettl, and F. Wang, Mott and generalized Wigner crystal states in WSe_2/WS_2 moiré superlattices, Nature **579**, 359 (2020).
[8] C. Jin, E. C. Regan, A. Yan, M. Iqbal Bakti Utama, D. Wang, S. Zhao, Y. Qin, S. Yang, Z. Zheng, S. Shi, K. Watanabe, T. Taniguchi, S. Tongay, A. Zettl, and F. Wang, Observation of moiré excitons in WSe_2/WS_2 heterostructure superlattices, Nature **567**, 76 (2019).
[9] K. L. Seyler, P. Rivera, H. Yu, N. P. Wilson, E. L. Ray, D. G. Mandrus, J. Yan, W. Yao, and X. Xu, Signatures of moiré-trapped valley excitons in $MoSe_2/WSe_2$ heterobilayers, Nature **567**, 66 (2019).
[10] K. Tran, G. Moody, F. Wu, X. Lu, J. Choi, K. Kim, A. Rai, D. A. Sanchez, J. Quan, A. Singh, J. Embley, A. Zepeda, M. Campbell, T. Autry, T. Taniguchi, K. Watanabe, N. Lu, S. K. Banerjee, K. L. Silverman, S. Kim, E. Tutuc, L. Yang, A. H. MacDonald, and X. Li, Evidence for moiré excitons in van der Waals heterostructures, Nature **567**, 71 (2019).
[11] Y. Cao, V. Fatemi, S. Fang, K. Watanabe, T. Taniguchi, E. Kaxiras, and P. Jarillo-Herrero, Unconventional superconductivity in magic-angle graphene superlattices, Nature **556**, 43 (2018).
[12] M. Yankowitz, S. Chen, H. Polshyn, Y. Zhang, K. Watanabe, T. Taniguchi, D. Graf, A. F. Young, and C. R. Dean, Tuning superconductivity in twisted bilayer graphene, Science **363**, 1059 (2019).
[13] G. Chen, A. L. Sharpe, P. Gallagher, I. T. Rosen, E. J. Fox, L. Jiang, B. Lyu, H. Li, K. Watanabe, T. Taniguchi, J. Jung, Z. Shi, D. Goldhaber-Gordon, Y. Zhang, and F. Wang, Signatures of tunable superconductivity in a trilayer graphene moiré superlattice, Nature **572**, 215 (2019).
[14] H. Ge, M. Yang, C. Ma, M.-H. Lu, Y.-F. Chen, N. Fang, and P. Sheng, Breaking the barriers: Advances in acoustic functional materials, National Science Review **5**, 159 (2018).
[15] V. Peri, M. Serra-Garcia, R. Ilan, and S. D. Huber, Axial-field-induced chiral channels in an acoustic Weyl system, Nature Physics **15**, 357 (2019).
[16] M. Serra-Garcia, V. Peri, R. Süsstrunk, O. R. Bilal, T. Larsen, L. G. Villanueva, and S. D. Huber, Observation of a phononic quadrupole topological insulator, Nature **555**, 342 (2018).
[17] X. Ni, M. Weiner, A. Alù, and A. B. Khanikaev, Observation of higher-order topological acoustic states protected by generalized chiral symmetry, Nature Materials **18**, 113 (2019).
[18] V. Peri, Z.-D. Song, M. Serra-Garcia, P. Engeler, R. Queiroz, X. Huang, W. Deng, Z. Liu, B. A. Bernevig, and S. D. Huber, Experimental characterization of fragile topology in an acoustic metamaterial, Science **367**, 797 (2020).
[19] J. Mei, Y. Wu, C. T. Chan, and Z.-Q. Zhang, First-principles study of Dirac and Dirac-like cones in phononic and photonic crystals, Physical Review B **86**, 035141 (2012).
[20] D. Torrent and J. Sánchez-Dehesa, Acoustic Analogue of Graphene: Observation of Dirac Cones in Acoustic Surface Waves, Physical Review Letters **108**, 174301 (2012).
[21] J. Lu, C. Qiu, S. Xu, Y. Ye, M. Ke, and Z. Liu, Dirac cones in two-dimensional artificial crystals for classical waves, Physical Review B **89**, 134302 (2014).
[22] S.-Y. Yu, X.-C. Sun, X. Ni, Q. Wang, X.-J. Yan, C. He, X.-P. Liu, L. Feng, M.-H. Lu, and Y.-F. Chen, Surface phononic graphene, Nature Materials **15**, 1243 (2016).
[23] D. Torrent, D. Mayou, and J. Sánchez-Dehesa, Elastic analog of graphene: Dirac cones and edge states for flexural waves in thin plates, Physical Review B **87**, 115143 (2013).
[24] T. Kariyado and Y. Hatsugai, Manipulation of Dirac Cones in Mechanical Graphene, Scientific Reports **5**, 18107 (2016).
[25] J. Lu, C. Qiu, W. Deng, X. Huang, F. Li, F. Zhang, S. Chen, and Z. Liu, Valley topological phases in bilayer sonic crystals, Physical Review Letters **120**, 116802 (2018).
[26] W. Dorrell, H. Pirie, S. M. Gardezi, N. C. Drucker, and J. E. Hoffman, van der Waals Metamaterials, Physical Review B **101**, 121103(R) (2020).
[27] M. Rosendo López, F. Peñaranda, J. Christensen, and P. San-Jose, Flat bands in magic-angle vibrating plates, Phys. Rev. Lett. **125**, 214301 (2020).
[28] Y. Deng, M. Oudich, N. J. Gerard, J. Ji, M. Lu, and Y. Jing, Magic-angle bilayer phononic graphene, Phys. Rev. B **102**, 180304 (2020).
[29] P. Wang, Y. Zheng, X. Chen, C. Huang, Y. V. Kartashov, L. Torner, V. V. Konotop, and F. Ye, Localization and delocalization of light in photonic moiré lattices, Nature **577**, 42 (2020).
[30] R. Bistritzer and A. H. MacDonald, Moiré bands in twisted double-layer graphene, Proc. Natl. Acad. Sci. USA **103**, 12233 (2011).
[31] K. H. Matlack, M. Serra-Garcia, A. Palermo, S. D. Huber, and C. Daraio, Designing perturbative metamaterials from discrete models, Nature Materials **17**, 323 (2018).
[32] E. Kogan and U. V. Nazarov, Symmetry classification of energy bands in graphene, Physical Review B **85**, 115418 (2012).
[33] P. L. de Andres, R. Ramírez, and J. A. Vergés, Strong covalent bonding between two graphene layers, Physical Review B **77**, 045403 (2008).
[34] E. McCann and M. Koshino, The electronic properties of bilayer graphene, Reports on Progress in Physics **76**, 056503 (2013).
[35] S. Shallcross, S. Sharma, E. Kandelaki, and O. A. Pankratov, Electronic structure of turbostratic graphene, Physical Review B **81**, 165105 (2010).
[36] P. Moon and M. Koshino, Optical Absorption in Twisted Bilayer Graphene, Physical Review B **87**, 205404 (2013).
[37] E. Suárez Morell, J. D. Correa, P. Vargas, M. Pacheco, and Z. Barticevic, Flat bands in slightly twisted bilayer graphene: Tight-binding calculations, Physical Review B **82**, 121407(R) (2010).
[38] S. Carr, S. Fang, Z. Zhu, and E. Kaxiras, Exact continuum model for low-energy electronic states of twisted bilayer graphene, Phys. Rev. Research **1**, 013001 (2019).
[39] K. Kim, A. DaSilva, S. Huang, B. Fallahazad, S. Larentis, T. Taniguchi, K. Watanabe, B. J. LeRoy, A. H. MacDonald, and E. Tutuc, Tunable moiré bands and strong correlations in small-twist-angle bilayer graphene, Proc. Natl. Acad. Sci. USA **114**, 3364 (2017).

[40] S. Carr, S. Fang, P. Jarillo-Herrero, and E. Kaxiras, Pressure dependence of the magic twist angle in graphene superlattices, Physical Review B **98**, 085144 (2018).

[41] L. Xian, D. M. Kennes, N. Tancogne-Dejean, M. Altarelli, and A. Rubio, Multiflat bands and strong correlations in twisted bilayer boron nitride: Doping-induced correlated insulator and superconductor, Nano Letters **19**, 4934 (2019).

[42] M. H. Naik and M. Jain, Ultraflatbands and shear solitons in moiré patterns of twisted bilayer transition metal dichalcogenides, Phys. Rev. Lett. **121**, 266401 (2018).

[43] T. Kariyado and A. Vishwanath, Flat band in twisted bilayer bravais lattices, Phys. Rev. Research **1**, 033076 (2019).

[44] G. Tarnopolsky, A. J. Kruchkov, and A. Vishwanath, Origin of magic angles in twisted bilayer graphene, Phys. Rev. Lett. **122**, 106405 (2019).

[45] M. Angeli, D. Mandelli, A. Valli, A. Amaricci, M. Capone, E. Tosatti, and M. Fabrizio, Emergent D_6 symmetry in fully relaxed magic-angle twisted bilayer graphene, Physical Review B **98**, 235137 (2018).

[46] H. Yoo, R. Engelke, S. Carr, S. Fang, K. Zhang, P. Cazeaux, S. H. Sung, R. Hovden, A. W. Tsen, T. Taniguchi, K. Watanabe, G.-C. Yi, M. Kim, M. Luskin, E. B. Tadmor, E. Kaxiras, and P. Kim, Atomic and electronic reconstruction at the van der Waals interface in twisted bilayer graphene, Nature Materials **18**, 448 (2019).

[47] M. Koshino and Y.-W. Son, Moiré phonons in twisted bilayer graphene, Physical Review B **100**, 075416 (2019).

[48] M. Lamparski, B. Van Troeye, and V. Meunier, Soliton signature in the phonon spectrum of twisted bilayer graphene, 2D Materials **7**, 025050 (2020).

[49] Z. Zhu, S. Carr, D. Massatt, M. Luskin, and E. Kaxiras, Twisted trilayer graphene: A precisely tunable platform for correlated electrons, Phys. Rev. Lett. **125**, 116404 (2020).

[50] K. J. Satzinger, Y. P. Zhong, H.-S. Chang, G. A. Peairs, A. Bienfait, M.-H. Chou, A. Y. Cleland, C. R. Conner, É. Dumur, J. Grebel, I. Gutierrez, B. H. November, R. G. Povey, S. J. Whiteley, D. D. Awschalom, D. I. Schuster, and A. N. Cleland, Quantum control of surface acoustic-wave phonons, Nature **563**, 661 (2018).

[51] Y. Chu, P. Kharel, T. Yoon, L. Frunzio, P. T. Rakich, and R. J. Schoelkopf, Creation and control of multi-phonon Fock states in a bulk acoustic-wave resonator, Nature **563**, 666 (2018).

[52] S. Fang and E. Kaxiras, Electronic structure theory of weakly interacting bilayers, Phys. Rev. B **93**, 235153 (2016).

Supplementary material

Simulating twistronics in acoustic metamaterials

S. Minhal Gardezi, Harris Pirie, Stephen Carr, William Dorrell, and Jennifer E. Hoffman
(Dated: March 24, 2021)

QUANTUM MIMICS

At first glance, the Newtonian behavior of sound seems completely detached from the quantum motion of electrons in solids. Yet at their heart, both systems follow straightforward wave equations: the Schrödinger equation for electrons and the acoustic wave equation for sound. The similarity between these wave equations allows some ideas to be translated between quantum mechanics and acoustics, provided the mapping is defined precisely. For example, the hydrogen-like solutions of the Schrödinger equation can be directly compared to the series of standing modes in an air cavity. Coupling two of these modes gives the same bonding and anti-bonding eigenmodes in acoustics as it does in quantum mechanics. In the main text, we implement this coupling acoustically via a channel that connects two cylindrical air cavities. But we push the analogy between acoustics and electronics even further: if we can imitate bonding and anti-bonding modes using two air cavities, can a sufficiently complex acoustic system mimic the emergent, collective behavior of thousands of electrons in a solid? Surprisingly, the answer is yes. Using two perforated steel plates coupled by a thin sheet of plastic, we precisely replicated in an *acoustic* system the low-energy *electronic* band structure of the quantum system of twisted bilayer graphene (TBG). Our metamaterial reshapes the flow of sound to mimic the localized behavior of electrons in magic-angle TBG. Importantly, our acoustic metamaterial design has a direct mapping to the tight-binding model that describes its quantum counterpart: each atom is represented by a single cavity, whose radius defines the band center E_D; hopping between cavities is implemented by channels, whose width defines the bandwidth $2t$; and hopping between layers is mediated by a plastic membrane, whose thickness controls the coupling 2Δ.

Yet, the analogy between acoustics and electronics has its limitations. First, our pressure eigenmodes are fundamentally bosonic, meaning they commute under exchange, unlike electrons. Consequently, we expect the interactions between our modes to be implemented differently from the interactions between electrons. But this fact doesn't prevent our metamaterial from recreating the single-particle eigenstates of its quantum counterpart. Second, our pressure fields are entirely classical, although recent experiments have demonstrated control of surface acoustic waves in the quantum limit [1, 2], and lattice geometries are a natural extension [3]. Despite these limitations, acoustic metamaterials have been designed to successfully imitate numerous electronic materials, including van der Waals heterostructures [4], higher-order topological insulators [5, 6], fragile topological states [7], and Weyl semimetals [8–10]—often demonstrating by analogy the novel properties of quantum systems *before* the quantum materials are first synthesized.

ROADMAP TO COMPLEX TWISTRONIC DEVICES

Currently, our metamaterial design provides a *computational platform* for a broad class of twisted vdW heterostructures, allowing the flat bands found in TBG (step 1 in Fig. S1) to be accurately mimicked in acoustics (step 2 in Fig. S1). It offers a different vantage point to view the nontrivial electronic phenomena found in TBG—one that strips away quantum-mechanical effects, so that topological and geometric effects can be isolated and understood.

In the longer term, 3D-printed acoustic metamaterials could offer a new way to *experimentally* simulate complex, multilayer vdW heterostructures with overlapping moiré patterns (step 3 in Fig. S1). Although today's electronic tight-binding calculations provide an accurate description of the moiré physics in bilayer honeycomb materials, such calculations are all but impossible in arbitrary multilayer structures with several independent twist angles [11]. Even the basic supercell is already generally nonexistent in trilayer graphene, due to the highly incommensurate beating of two bilayer moiré patterns [12]. Similar computation intractability arises when generalizing to lattice geometries beyond the honeycomb structure of graphene. Likewise, there are not clear paths forward in the theoretical modeling of a twist angle in more-general metallic or multi-band materials [13]. With experiments fast approaching this multilayer paradigm [14–16], new theoretical tools are urgently needed. And while *computational* acoustics suffers much the same limitations as tight-binding calculations, our work paves the way for *experimental* acoustic metamaterials to fill the gap between theory and next-generation quantum devices. Specifically, we demonstrate numerically that tabletop acoustic simulators of twisted vdW heterostructures mimic their quantum counterparts with sufficient

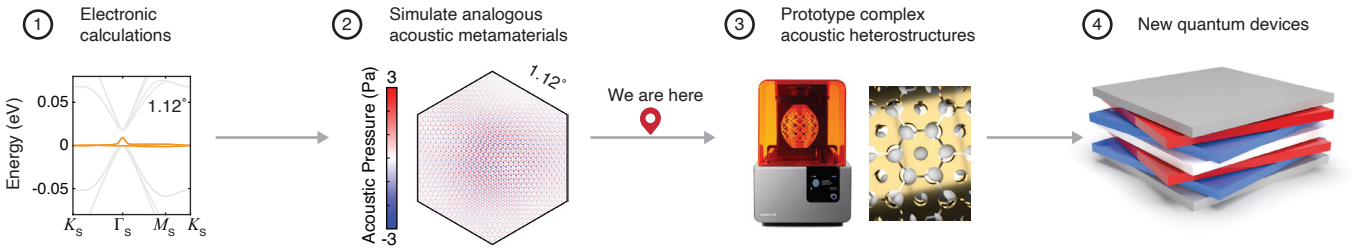

FIG. S1. Roadmap to complex twistronic devices. Acoustic metamaterials provide a stepping stone between today's electronic calculations and tomorrow's quantum devices.

precision to be useful experimental testbeds for quantum materials. The next step is to 3D print and measure an acoustic analog of TBG. Finally, our design scheme also applies to the length scales and materials required for surface-acoustic-wave devices or integrated photonics. In practice, these alternative platforms may provide an easier route to fabricate the large arrays required to explore general twisted vdW metamaterials.

We view acoustic metamaterials as a stepping stone between today's tight-binding calculations and tomorrow's quantum devices. Compared to theory, they allow the exploration of more general (e.g. multilayer, multiband, non-hexagonal, or variably-relaxed) twisted vdW systems, as described above. Compared to experiment, they overcome limitations like disorder in the local twist angle [17] or large-scale atomic relaxation [18], both of which have unavoidable, adverse effects on the ideal band structure and make some interesting geometries currently unaccessible. The enormous phase space of twisted vdW systems means there are likely many interesting phenomena yet to be explored, but with no practical way to do so. Acoustic metamaterials offer a clean platform to rapidly prototype these twistronic phases.

More broadly, quantum materials constitute a discrete set of possible physical systems: there are 82 reasonably stable elements on the periodic table and 230 space groups in which to arrange them. Within this vast space, moiré engineering has been contemplated in only a few material systems, including graphene, insulating hexagonal boron nitride [19], transition-metal dichalcogenides [20–22], magnetic chromium triiodide [23, 24], and black phosphorous. Even so, these few systems already host a diverse range of interesting phases. Yet, the discrete and limited nature of these material platforms hinders a broader exploration of twistronics—either theoretically or experimentally. In contrast, acoustic metamaterials offer the remarkable possibility to explore *intermediate compounds* because they can be tuned continuously. They bridge the gap between discrete material platforms, allowing their emergent properties to be isolated, optimized, or combined—informing future devices. For example, an acoustic analog of TBG could be smoothly deformed into an analog of twisted hexagonal boron nitride, allowing the evolution from twisted Dirac cones to twisted quadratic bands to be continuously studied.

[1] K. J. Satzinger, Y. P. Zhong, H.-S. Chang, G. A. Peairs, A. Bienfait, M.-H. Chou, A. Y. Cleland, C. R. Conner, É. Dumur, J. Grebel, I. Gutierrez, B. H. November, R. G. Povey, S. J. Whiteley, D. D. Awschalom, D. I. Schuster, and A. N. Cleland, Quantum control of surface acoustic-wave phonons, Nature **563**, 661 (2018).

[2] Y. Chu, P. Kharel, T. Yoon, L. Frunzio, P. T. Rakich, and R. J. Schoelkopf, Creation and control of multi-phonon Fock states in a bulk acoustic-wave resonator, Nature **563**, 666 (2018).

[3] S.-Y. Yu, X.-C. Sun, X. Ni, Q. Wang, X.-J. Yan, C. He, X.-P. Liu, L. Feng, M.-H. Lu, and Y.-F. Chen, Surface phononic graphene, Nature Materials **15**, 1243 (2016).

[4] W. Dorrell, H. Pirie, S. M. Gardezi, N. C. Drucker, and J. E. Hoffman, van der Waals Metamaterials, Physical Review B **101**, 121103(R) (2020).

[5] M. Serra-Garcia, V. Peri, R. Süsstrunk, O. R. Bilal, T. Larsen, L. G. Villanueva, and S. D. Huber, Observation of a phononic quadrupole topological insulator, Nature **555**, 342 (2018).

[6] X. Ni, M. Weiner, A. Alù, and A. B. Khanikaev, Observation of higher-order topological acoustic states protected by generalized chiral symmetry, Nature Materials **18**, 113 (2019).

[7] V. Peri, Z.-D. Song, M. Serra-Garcia, P. Engeler, R. Queiroz, X. Huang, W. Deng, Z. Liu, B. A. Bernevig, and S. D. Huber, Experimental characterization of fragile topology in an acoustic metamaterial, Science **367**, 797 (2020).

[8] F. Li, X. Huang, J. Lu, J. Ma, and Z. Liu, Weyl points and Fermi arcs in a chiral phononic crystal, Nature Physics **14**, 30 (2017).

[9] H. He, C. Qiu, L. Ye, X. Cai, X. Fan, M. Ke, F. Zhang, and Z. Liu, Topological negative refraction of surface acoustic waves in a Weyl phononic crystal, Nature **560**, 61 (2018).

[10] B. Xie, H. Liu, H. Cheng, Z. Liu, S. Chen, and J. Tian, Experimental Realization of Type-II Weyl Points and Fermi Arcs in Phononic Crystal, Physical Review Letters **122**, 104302 (2019).

[11] S. Carr, S. Fang, and E. Kaxiras, Electronic-structure methods for twisted moiré layers, Nature Reviews Materials **5**, 748 (2020).

[12] Z. Zhu, S. Carr, D. Massatt, M. Luskin, and E. Kaxiras, Twisted trilayer graphene: A precisely tunable platform for correlated electrons, Phys. Rev. Lett. **125**, 116404 (2020).

[13] S. Carr, D. Massatt, M. Luskin, and E. Kaxiras, Duality between atomic configurations and Bloch states in twistronic materials, Physical Review Research **2**, 033162 (2020).

[14] G. Chen, A. L. Sharpe, P. Gallagher, I. T. Rosen, E. J. Fox, L. Jiang, B. Lyu, H. Li, K. Watanabe, T. Taniguchi, J. Jung, Z. Shi, D. Goldhaber-Gordon, Y. Zhang, and F. Wang, Signatures of tunable superconductivity in a trilayer graphene moiré superlattice, Nature **572**, 215 (2019).

[15] C. Shen, Y. Chu, Q. Wu, N. Li, S. Wang, Y. Zhao, J. Tang, J. Liu, J. Tian, K. Watanabe, T. Taniguchi, R. Yang, Z. Y. Meng, D. Shi, O. V. Yazyev, and G. Zhang, Correlated states in twisted double bilayer graphene, Nature Physics **16**, 520 (2020).

[16] Y. Cao, D. Rodan-Legrain, O. Rubies-Bigorda, J. M. Park, K. Watanabe, T. Taniguchi, and P. Jarillo-Herrero, Tunable correlated states and spin-polarized phases in twisted bilayer–bilayer graphene, Nature **583**, 215 (2020).

[17] A. Uri, S. Grover, Y. Cao, J. A. Crosse, K. Bagani, D. Rodan-Legrain, Y. Myasoedov, K. Watanabe, T. Taniguchi, P. Moon, M. Koshino, P. Jarillo-Herrero, and E. Zeldov, Mapping the twist-angle disorder and Landau levels in magic-angle graphene, Nature **581**, 47 (2020).

[18] H. Yoo, R. Engelke, S. Carr, S. Fang, K. Zhang, P. Cazeaux, S. H. Sung, R. Hovden, A. W. Tsen, T. Taniguchi, K. Watanabe, G.-C. Yi, M. Kim, M. Luskin, E. B. Tadmor, E. Kaxiras, and P. Kim, Atomic and electronic reconstruction at the van der Waals interface in twisted bilayer graphene, Nature Materials **18**, 448 (2019).

[19] L. Xian, D. M. Kennes, N. Tancogne-Dejean, M. Altarelli, and A. Rubio, Multiflat Bands and Strong Correlations in Twisted Bilayer Boron Nitride: Doping-Induced Correlated Insulator and Superconductor, Nano Letters **19**, 4934 (2019).

[20] F. Wu, T. Lovorn, and A. H. MacDonald, Topological Exciton Bands in Moiré Heterojunctions, Physical Review Letters **118**, 147401 (2017).

[21] K. Tran, G. Moody, F. Wu, X. Lu, J. Choi, K. Kim, A. Rai, D. A. Sanchez, J. Quan, A. Singh, J. Embley, A. Zepeda, M. Campbell, T. Autry, T. Taniguchi, K. Watanabe, N. Lu, S. K. Banerjee, K. L. Silverman, S. Kim, E. Tutuc, L. Yang, A. H. MacDonald, and X. Li, Evidence for moiré excitons in van der Waals heterostructures, Nature **567**, 71 (2019).

[22] C. Jin, E. C. Regan, A. Yan, M. Iqbal Bakti Utama, D. Wang, S. Zhao, Y. Qin, S. Yang, Z. Zheng, S. Shi, K. Watanabe, T. Taniguchi, S. Tongay, A. Zettl, and F. Wang, Observation of moiré excitons in WSe_2/WS_2 heterostructure superlattices, Nature **567**, 76 (2019).

[23] P. Jiang, C. Wang, D. Chen, Z. Zhong, Z. Yuan, Z.-Y. Lu, and W. Ji, Stacking tunable interlayer magnetism in bilayer CrI_3, Physical Review B **99**, 144401 (2019).

[24] K. Zollner, P. E. Faria Junior, and J. Fabian, Proximity exchange effects in $MoSe_2$ and WSe_2 heterostructures with CrI_3: Twist angle, layer, and gate dependence, Physical Review B **100**, 085128 (2019).